

Capacitive Detection of Low-Enthalpy, Higher-Order Phase Transitions in Synthetic and Natural Composition Lipid Membranes

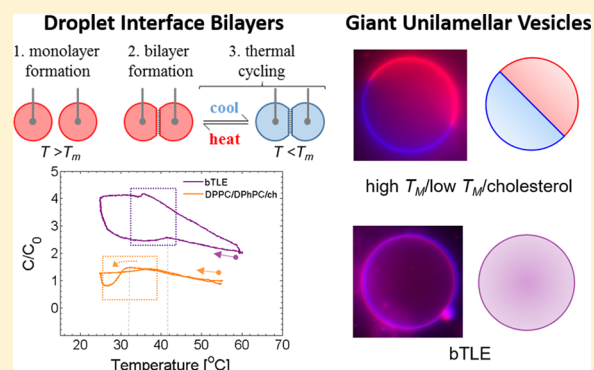
Graham J. Taylor,^{†,||} Frederick A. Heberle,^{||,⊥} Jason S. Seinfeld,[†] John Katsaras,^{⊥,#,§}
C. Patrick Collier,^{*,†,||,∇} and Stephen A. Sarles^{*,†}

[†]Department of Mechanical, Aerospace, and Biomedical Engineering, and [§]Department of Physics and Astronomy, The University of Tennessee, Knoxville, Tennessee 37996, United States

^{||}Joint Institute for Biological Sciences, [⊥]Biology and Soft Matter Division, [#]Shull Wollan Center—A Joint Center for Neutron Sciences, and [∇]Center for Nanophase Materials Sciences, Oak Ridge National Laboratory, Oak Ridge, Tennessee 37831, United States

Supporting Information

ABSTRACT: In-plane lipid organization and phase separation in natural membranes play key roles in regulating many cellular processes. Highly cooperative, first-order phase transitions in model membranes consisting of few lipid components are well understood and readily detectable via calorimetry, densitometry, and fluorescence. However, far less is known about natural membranes containing numerous lipid species and high concentrations of cholesterol, for which thermotropic transitions are undetectable by the above-mentioned techniques. We demonstrate that membrane capacitance is highly sensitive to low-enthalpy thermotropic transitions taking place in complex lipid membranes. Specifically, we measured the electrical capacitance as a function of temperature for droplet interface bilayer model membranes of increasing compositional complexity, namely, (a) a single lipid species, (b) domain-forming ternary mixtures, and (c) natural brain total lipid extract (bTLE). We observed that, for single-species lipid bilayers and some ternary compositions, capacitance exhibited an abrupt, temperature-dependent change that coincided with the transition detected by other techniques. In addition, capacitance measurements revealed transitions in mixed-lipid membranes that were not detected by the other techniques. Most notably, capacitance measurements of bTLE bilayers indicated a transition at ~ 38 °C not seen with any other method. Likewise, capacitance measurements detected transitions in some well-studied ternary mixtures that, while known to yield coexisting lipid phases, are not detected with calorimetry or densitometry. These results indicate that capacitance is exquisitely sensitive to low-enthalpy membrane transitions because of its sensitivity to changes in bilayer thickness that occur when lipids and excess solvent undergo subtle rearrangements near a phase transition. Our findings also suggest that heterogeneity confers stability to natural membranes that function near transition temperatures by preventing unwanted defects and macroscopic demixing associated with high-enthalpy transitions commonly found in simpler mixtures.



INTRODUCTION

The lipid raft hypothesis posits that the lateral organization of lipids in cell membranes plays an important role in processes such as protein sorting, signaling, exocytosis and endocytosis, membrane–protein organization and function, and the attachment and coordination of cytoskeletal filaments.^{1–6} To date, much is known about the fundamental phase behaviors of lipids and the thermotropic transitions of membranes composed of one or a few types of lipids. In these simplified model systems, researchers have established the thermodynamics and energetics associated with different lipid phase transitions. These range from chain-melting transitions in single-component lipid bilayers to miscibility transitions in multicomponent lipid mixtures. The latter include the coexistence of liquid-ordered (Lo) and liquid-disordered (Ld) phases in certain three- and four-component mixtures containing cholesterol that are often

used to model the eukaryotic plasma membrane.¹ However, natural cell membranes are composed of tens to hundreds of different lipid species,⁷ and it remains unclear how this extreme heterogeneity affects the spatial organization of species in the plasma membrane. Although a number of studies have examined the thermotropic behaviors of prokaryotic (mycoplasma *Acholeplasma laidlawii* or *E. coli*) membranes and membrane extracts,^{8–14} there are few reports of phase and miscibility transitions in cholesterol-containing eukaryotic lipid membranes.¹⁵

Specific capacitance (C_M), defined as the electrical capacitance per unit area, is an intrinsic membrane property

Received: June 15, 2017

Revised: August 11, 2017

Published: August 15, 2017

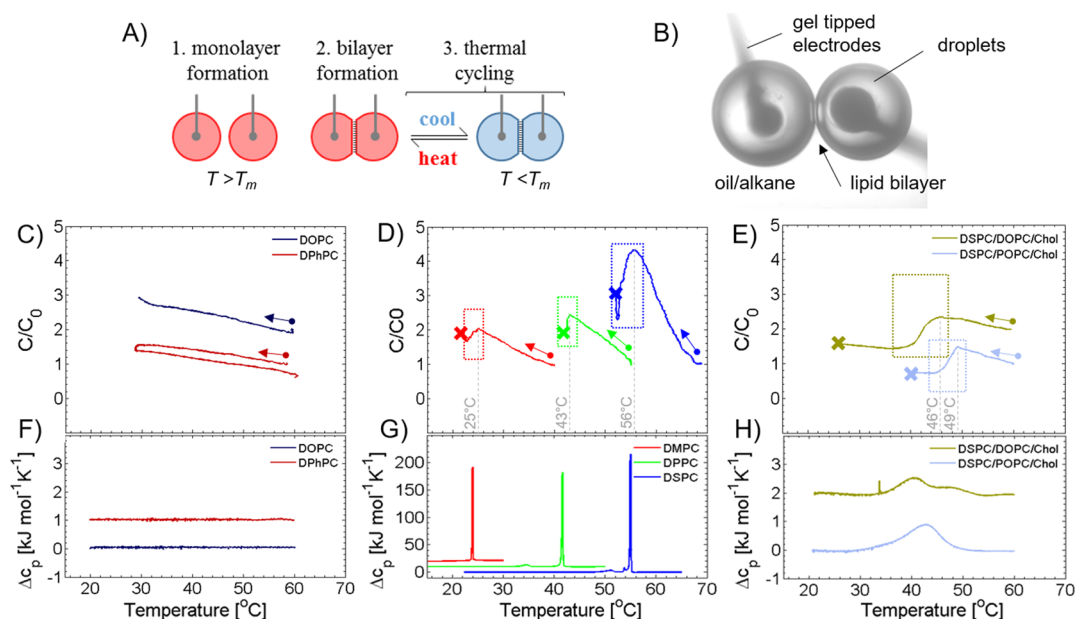


Figure 1. Phase transitions in droplet interface bilayers (DIBs) revealed by electrical capacitance measurements. (A) Schematic illustration of DIB formation. (B) Image of DIB formation at the interface between two contacting water droplets suspended in alkane solvent. Each droplet contains large unilamellar vesicles of the desired bilayer composition that spontaneously adsorb to the oil/water interface to form a monolayer. (C–E) Representative capacitance vs temperature (C – T) curves obtained while cooling DIBs formed from different lipid compositions as indicated in the legends. Ternary compositions in (E, H) were DSPC/DOPC/Chol or DSPC/POPC/Chol at 39/39/22 mol %. Arrows with circular end points indicate the starting temperature, and transition regions are enclosed by dashed boxes. For (D) and (E), bilayer rupture is indicated by an X, and traces were selected that show the full capacitive response (without rupture) between local maxima and minima. Alkane solvents: C10 (DMPC), C12 (DPPC), C14 (DSPC), and C16 (DOPC, DPhPC, ternary mixtures). (F–H) Excess molar heat capacity vs temperature obtained from DSC measurements of MLVs in water. Both C – T and DSC curves are offset vertically for clarity.

that is proportional to the bilayer dielectric permittivity and inversely proportional to its thickness. Because the acyl chain composition and orientation in the membrane affect the permittivity and thickness, C_M is directly influenced by the membrane composition and thermotropic phase. Although many studies have shown that electrical capacitance is sensitive to thermally induced lipid phase transitions in single-component model membranes,^{16–21} few capacitance measurements have been reported for lipid mixtures. Langner et al. used capacitance measurements and electron spin resonance spectroscopy to detect a suspected phase transition in a bilayer assembled from red blood cell total lipid extract.¹⁵ However, they did not discuss the mechanism of the associated transition or the sensitivity of capacitance measurements to the transition. In other work, Naumowicz and Figaszewski measured the specific capacitance of membranes formed from binary mixtures of phosphatidylcholine (PC) and small molecules.^{22–27} However, the scope of the authors' studies did not consider temperature-induced changes in the membrane structure or thermotropic phase. To our knowledge, capacitance measurements have not been conducted on three- or four-component cholesterol-containing mixtures that have recently gained attention as tractable models for phase separation and lipid raft formation across a range of length scales.²⁸ As such, there is yet untapped potential to use capacitance measurements for examining thermal transitions occurring in multicomponent membranes that more closely reflect the lipid heterogeneity found in cells.

Studying the phase behavior in complex mixtures is a difficult task, and a variety of different tools and methods are needed to perform such studies. Nuclear magnetic resonance (NMR), small-angle neutron scattering (SANS), and atomic force

microscopy (AFM) have been used to study phase transitions in single-component²⁹ and ternary-phase separating membrane systems.^{30,31} However, there are notable limitations to these approaches. ²H NMR and SANS investigation of phase separation require that at least one lipid type be selectively perdeuterated,^{30,31} and it is difficult to achieve such selective perdeuteration³² in complex mixtures and total lipid extracts that contain many lipid types. AFM has been used extensively to image phase separation in lipid bilayers formed by vesicle deposition onto solid surfaces. Unfortunately, solid-supported membranes often exhibit defects³³ (i.e., incomplete surface coverage) and altered physical properties^{34–37} compared to aqueous vesicle membranes and freestanding lipid bilayers. Thus, there exists significant opportunity for capacitance measurements to complement these approaches to studying membrane phase behaviors.

Here, we present measurements of the temperature-dependent electrical capacitance in planar bilayers composed of synthetic single- or three-component lipid mixtures or natural brain total lipid extract (bTLE). We used the droplet interface bilayer (DIB) technique³⁸ to construct stable lipid bilayers between lipid-coated water droplets immersed in alkane oil. DIBs are well suited for this study because they allow independent measurements of nominal membrane capacitance and the bilayer area (i.e., contact area between two droplets), thereby enabling a precise determination of C_M .^{39,40} Our experiments with single-component DIBs confirm the findings of previous reports on homogeneous bilayers formed in the presence of excess alkane solvent,^{16–21} namely that capacitance measurements can detect the phase transitions of saturated lipid membranes at the same temperatures as those assessed on oil-free liposomes using methods such as differential scanning

Table 1. Capacitive Transition Temperature Limits and Widths for DIBs with Varying Lipid Compositions

lipid	$T_{\text{lower}}/T_{\text{upper}}$ (°C)	ΔT (°C)	T_M (°C)	T_M^c (°C)
DPhPC				<−120 ⁴²
DOPC				−18 ²⁹
DMPC	23/25	2	24	23.9/23.7 ^{41,50}
DPPC	41/43	2	42	41.4 ⁴¹
DSPC	53/56	3	54–55	55.3 ⁴¹
DSPC/DOPC/Chol ^a	37/46	9	41–42	40–50 ⁴⁵
DSPC/POPC/Chol ^a	43/49	8	46	40–50 ⁴⁵
DPPC/DPhPC/Chol ^b	26/32	6	29	28–33 ³¹
bTLE	35/42	7	38–39	not known

^a39/39/22 mol %. ^b20/50/30 mol %. ^cFrom the literature.

calorimetry. However, for the first time we find that capacitance measurements of bilayers containing mixtures of synthetic or natural lipids reveal subtle, temperature-dependent lipid rearrangements that are not detected by the other techniques mentioned. Our results also show the mechanism that imparts the extraordinary sensitivity of capacitance measurements to phase transitions as being the result of an entropically driven reorganization of both the lipids and residual alkane solvent in the membrane.

RESULTS

Capacitance measurements were performed at temperatures between ambient (~ 25 °C) and 60 °C on single- and multicomponent DIBs. Single-component systems included saturated DMPC, DPPC, and DSPC bilayers (see [Methods and Materials](#) for details), which undergo well-characterized first-order chain-melting transitions (T_M) in the temperature range studied herein.⁴¹ As controls, we examined DOPC and DPhPC bilayers, which melt at -17.3 °C²⁹ and <-120 °C,⁴² respectively, and therefore remain in a liquid-crystalline phase in our experiments. We also examined synthetic lipid bilayers formed from ternary mixtures composed of a high-melting lipid (saturated DPPC or DSPC), a low-melting lipid (unsaturated POPC or DOPC, or highly-branched DPhPC), and cholesterol (Chol). These mixtures separate into liquid-ordered (Lo) and liquid-disordered (Ld) phases below a miscibility transition temperature, T_{misc} , as observed previously.^{31,43–45} Finally, we characterized the temperature-dependent capacitance of DIBs assembled from bTLE, a natural lipid mixture whose thermotropic behavior is less well studied. Like the ternary models that mimic raft formation, bTLE is rich in high-melting lipids (most notably, sphingomyelins), low-melting mixed-chain lipids, and cholesterol (see [SI Figure S2](#) for the bTLE acyl chain composition). In parallel with these measurements on planar lipid bilayers, we characterized multilamellar vesicles (MLVs) formed from the same lipid compositions using differential scanning calorimetry (DSC), pressure perturbation calorimetry (PPC), and densitometry.

Electrical Capacitance Is Sensitive to Lipid Melting and Miscibility Transitions. For single-component saturated and ternary mixed membranes, we found that stable DIBs formed only when the droplets were connected in a reservoir of oil at a temperature above T_M or T_{misc} . This finding is consistent with a previous report that contacting droplets will coalesce unless monolayer assembly can occur at a temperature above T_M .⁴⁶ After incubating two 300 nL droplets at elevated temperature (50–60 °C), the droplets were brought into contact to facilitate the spontaneous formation of a lipid bilayer ([Figure 1A,B](#)). An additional 3–5 min was allowed for the

capacitance and area of the bilayer to equilibrate before commencing capacitance measurements as a function of temperature (cooling and heating cycles).

[Figure 1C–E](#) shows representative capacitance-temperature ($C-T$) responses obtained from different synthetic lipid DIB compositions, where C/C_0 is the nominal bilayer capacitance (C) normalized by its initial value (C_0) measured in the heated state. Representative DSC thermograms are shown in the lower panel of [Figure 1F–H](#). PPC and densitometry results are included in the [Supporting Information](#) ([Figure S1](#)). The temperature-dependent capacitance of single-component membranes displayed one of two main characteristic responses (i.e., linear or nonlinear), depending on whether the membrane was cooled through T_M . The nominal capacitance of DPhPC and DOPC membranes increased monotonically with decreasing temperature and reversibly decreased upon heating, as shown in [Figure 1C](#). In contrast, the capacitance did not increase monotonically for single-component DIBs formed from saturated DMPC, DPPC, and DSPC lipids ([Figure 1D](#)). Instead, cooling these bilayers resulted in a three-part response: (a) capacitance first increased from its value in the heated state to a local maximum value at lower temperature; (b) cooling below this temperature caused the capacitance to decrease to a local minimum; and (c) further cooling caused the capacitance to increase again before spontaneous bilayer rupture and droplet coalescence occurred. Indeed, we found that saturated lipid bilayers ruptured once the temperature was decreased below T_M ($n > 3$ for each composition). Similar instability of single-component planar lipid bilayers has been observed by others.^{20,47} The midpoint, end points, and width of the transition region (indicated by dashed boxes in [Figure 1D](#)) are reported in [Table 1](#). For each saturated lipid, the midpoint of the local maximum and minimum in the $C-T$ curve coincides with T_M obtained from DSC measurements ([Figure 1G](#)). The agreement between the transition temperatures obtained from capacitance measurements of planar bilayers formed in the presence of alkane solvent and from DSC of solvent-free liposomes indicates that the chain-melting transition of saturated lipid bilayers was not significantly affected by residual solvent in the DIB. (Refer to the [Figure 1](#) caption for solvent types.)

We next examined the thermotropic response of DIBs formed from ternary lipid mixtures DSPC/DOPC/Chol and DSPC/POPC/Chol, both of which are known to undergo a temperature-dependent miscibility transition. $C-T$ responses obtained while cooling these DIBs ([Figure 1E](#)) exhibited transitions that were qualitatively similar to those seen in saturated single-component bilayers, with a local maximum and minimum in capacitance. As with saturated lipid DIBs, the

ternary DIBs ruptured within minutes after the temperature decreased below the apparent transition temperature ($n = 3$ for each composition). The transitions observed in DIB $C-T$ curves with the DSPC-based ternary mixtures occur at temperatures that agree with values of T_{misc} obtained from SANS⁴⁵ and fluorescence imaging³¹ of solvent-free, phase-separated vesicles and planar lipid bilayers^{48,49} containing residual solvent. This agreement suggests that the non-monotonic changes in bilayer capacitance near 45–50 °C are caused by the lateral reorganization of lipids and that the presence of hexadecane (C16) in the bilayer does not significantly affect this miscibility transition. The agreement between transition temperatures obtained from capacitance measurements (Table 1) and T_{misc} determined from small-angle neutron scattering data⁴⁵ is consistent with previous reports of similar phase behavior in planar and solvent-free ternary bilayer mixtures^{48,49} and suggests that the nonmonotonic changes in bilayer capacitance near 45–50 °C are caused by the lateral reorganization of lipids.

Low-Enthalpy Transitions in Synthetic and Natural Model Membranes. Figure 2A shows $C-T$ traces for DIBs

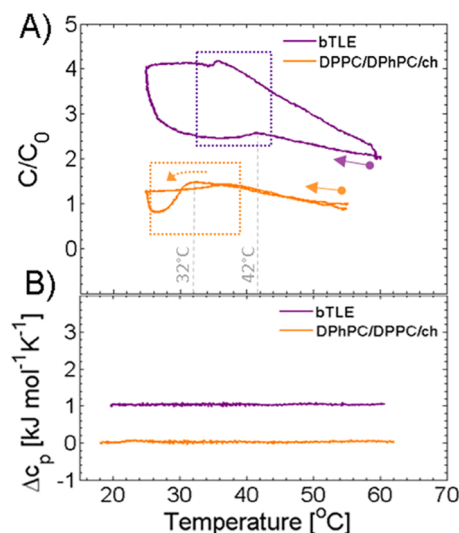


Figure 2. Low-enthalpy phase transitions revealed by electrical capacitance measurements. (A) $C-T$ curves obtained while cooling DPPC/DPhPC/Chol (20/50/30 mol %) and bTLE DIBs (C16 alkane solvent). Arrows with circular end points indicate the starting point of the cooling leg, and the dashed arrow indicates the cooling leg of the response. Transition regions are enclosed by dashed boxes. (B) Excess molar heat capacity of lipid vesicles dispersed in water.

formed from either bTLE or DPPC/DPhPC/Chol 20/50/30 mol %, a ternary mixture whose phase behavior has been extensively characterized with fluorescence microscopy and ²H NMR.^{31,48,51} For both mixtures, $C-T$ curves shown in Figure 2A showed a transition upon cooling. The transition temperature range for the DPPC/DPhPC/Chol DIB (Figure 2A, dashed orange box) agrees with the miscibility temperature ranges reported for planar bilayers^{48,49} and solvent-free giant unilamellar vesicles (GUVs)³¹ of the same composition. Unlike the ternary DSPC/DOPC/Chol and DSPC/POPC/Chol lipid mixtures (Figure 1E), DIBs formed from bTLE or DPPC/DPhPC/Chol remained intact upon cooling to ambient temperature and subsequent reheating. This stability enabled the measurement of a full $C-T$ loop (Figure 2A), including the observation of a change in the slope of C vs T during the

heating leg. The similar capacitive response of bTLE and a ternary domain-forming mixture strongly suggests that the natural mixture undergoes a lateral lipid reorganization between 35 and 42 °C.

Initial attempts to form bTLE DIBs at room temperature were unsuccessful because the droplets coalesced immediately upon contact. This observation suggests that sufficient monolayer assembly at the surfaces of the droplets was not achieved at room temperature. However, like DIBs assembled from DPPC or *E. coli* total lipid extract,⁴⁶ long-lasting bTLE bilayers were readily formed after 2 to 3 min of monolayer assembly at temperatures between 45 and 60 °C. The fact that bTLE DIB formation was unsuccessful at room temperature, but enabled by heating, also suggests that bTLE undergoes a lateral lipid reorganization between 35 and 42 °C and exists in a disordered fluid phase at higher temperatures.

DSC thermograms of DPPC/DPhPC/Chol liposomes (Figure 2B) showed no indication of the previously reported miscibility transition^{31,48} to which we attribute the ternary DIB $C-T$ transitions shown in Figure 2A. bTLE thermograms were similarly featureless, and indeed DSC, PPC, and density measurements (Figure 2B and Figure S1) all produced curves resembling those of single-phase membranes. These featureless thermograms indicate that the miscibility transitions of both DPPC/DPhPC/Chol (20/50/30 mol %) and the natural bTLE mixture are low-enthalpy transitions, i.e., $\Delta H \approx 0$, and potentially of a higher order.

bTLE Membranes Do Not Undergo a First-Order Phase Transition. To better understand the nature of the low-enthalpy capacitive transition observed in bTLE DIBs, we used fluorescence microscopy of GUVs and fluorescence resonance energy transfer (FRET) spectroscopy of LUVs to interrogate the size of phase domains. Figure 3 shows fluorescence micrographs of GUVs formed from DSPC/DOPC/Chol 39/39/22 mol % (Figure 3A), DSPC/POPC/Chol 39/39/22 mol % (Figure 3B), and bTLE (Figure 3C). Trace quantities of the fluorophores naphthopyrene (blue channel, Lo phase marker) and C12:0-DiI (red channel, Ld phase marker) allowed the visualization of coexisting Lo and Ld phases, respectively.⁵² In the DSPC/DOPC/Chol mixture, large phase-separated domains were clearly visible (Figure 3A). In contrast, GUVs composed of either DSPC/POPC/Chol 39/39/22 mol % or bTLE (Figure 3B,C) appeared homogeneous with no visible phase separation. Despite their apparent uniformity on the micrometer length scale, the lack of visible domains does not rule out the possibility of domains with sizes below the resolution limit of standard optical microscopy, i.e., <200 nm.

To investigate these mixtures on the nanoscopic length scale, we used FRET spectroscopy with 100 nm LUVs. FRET between fluorescent lipid analogs has been successfully used to detect domains as small as ~5 nm in lipid mixtures.^{53–56} Figure 3D–F shows the sensitized acceptor emission under conditions of donor excitation (steady-state probe-partitioning FRET⁵⁶) for a system with three probes comprising two energy-transfer pairs, i.e., DHE, which partitions favorably into cholesterol-rich Lo phases, and BoDIPY-PC and C12:0-DiI, which partition into disordered Ld phases.⁵⁴ Depending on the spatial proximity of these probes, excited-state DHE can transfer energy to BoDIPY-PC, and excited-state BoDIPY-PC can in turn transfer energy to DiI. In a phase-separated bilayer, the spatial segregation of DHE and BoDIPY-PC leads to a reduction in FRET efficiency for this donor/acceptor pair,

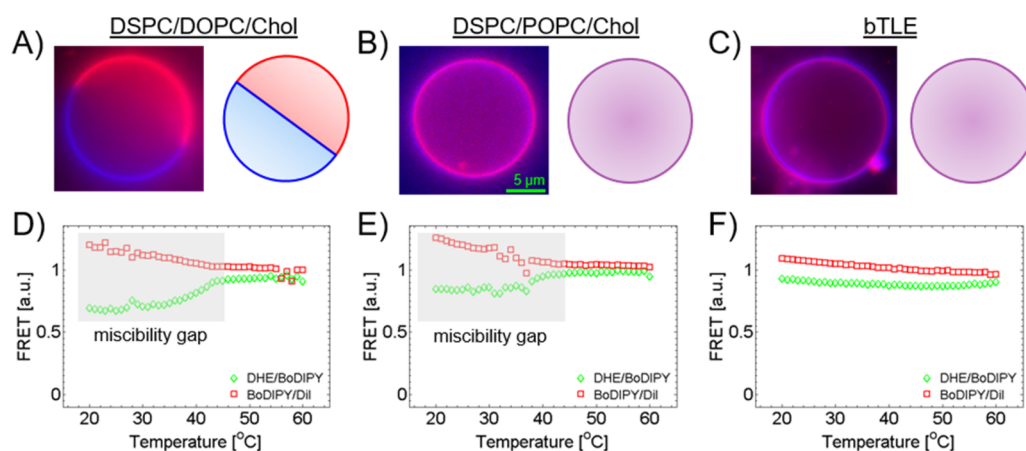


Figure 3. Phase domains are not detected in bTLE by microscopy or FRET. (A–C) Images obtained from fluorescence microscopy experiments used to determine the phase separation in DSPC/DOPC/Chol (39/39/22 mol %) (A), ternary DSPC/POPC/Chol (39/39/22 mol %) GUVs (B), and bTLE GUVs (C). GUV images were obtained at ambient temperature. Dyes: C12:0 DiI (red, prefers the Ld phase) and naphthopyrene (blue, prefers the Lo phase). Probe/lipid ratios were 1:1500 and 1:3000, respectively. (D–F) Results of a FRET-miscibility assay for thermotropic phase separation and miscibility transitions in mixtures of (D) DSPC/DOPC/Chol (39/39/22 mol %), (E) DSPC/POPC/Chol (39/39/22 mol %), and (F) bTLE.

whereas the colocalization of BoDIPY-PC and DiI leads to an increase in energy transfer. This phenomenon is easily seen for ternary mixtures DSPC/DOPC/Chol and DSPC/POPC/Chol (Figure 3D,E). For both mixtures, FRET of the DHE/BoDIPY-PC pair decreased as the temperature was lowered below T_{misc} , whereas FRET for the BoDIPY-PC/DiI pair increased, consistent with previous reports for these mixtures.^{53–55} Moreover, the upper miscibility temperature from FRET spectra (44 °C for DSPC/DOPC/Chol, 43 °C for DSPC/POPC/Chol) falls within 3–6 °C of the T_{upper} value obtained from DIB C – T curves (Table 1). In contrast, FRET in the bTLE mixture does not show abrupt changes for either probe pair (Figure 3F), suggesting that this mixture is laterally homogeneous on the >5 nm length scale.

DIB Capacitance Is Sensitive to Alkane Solvent Reorganization at the Phase Transition. To elucidate the physical mechanisms underlying the capacitive transition observed in DIBs, we performed specific capacitance and electrowetting measurements. Results from these measurements are found in Figures 4 and 5, respectively.

In contrast to the monotonic behavior observed for fluid-phase DPhPC/hexadecane, the specific capacitance of the bTLE/hexadecane DIB showed nonlinear behavior that resembled the cooling leg of its nominal C – T curve (Figure 2A). C_M first increased monotonically to a local maximum upon cooling from 60 to 43 °C, followed by a decrease to a local minimum at 39 °C and then another monotonic increase upon further reduction in temperature. For both bTLE and DPhPC, the overall trend is a decreasing specific capacitance with increasing temperature (Figure 4A). Because the bilayer hydrocarbon thickness d_{HC} is inversely proportional to C_M , this result indicates that heating thickens the DPhPC membrane. The observed heating-induced thickening is consistent with the trend observed on glycerol monooleate bilayers formed in the presence of alkanes;^{18,57} however, it is opposite to the trend found for DPhPC (and indeed all fluid-phase glycerophospholipids) in solvent-free liposomes, where increased temperature results in a larger area per lipid and a smaller hydrophobic thickness.⁵⁸

We then assembled and characterized bTLE DIBs in heptadecane (C17), a longer-chain alkane expected to yield

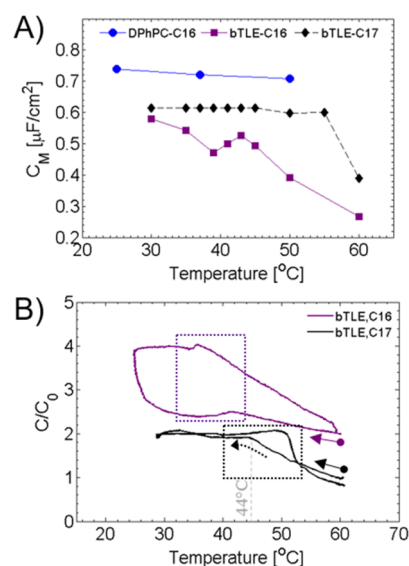


Figure 4. Capacitive transition in DIBs is influenced by alkane solvent. (A) Specific capacitance, C_M was measured at various temperatures with DPhPC and bTLE DIBs formed in hexadecane (C16) or heptadecane (C17). (B) Normalized nominal C – T curves from bTLE DIBs in C16 (same as in Figure 2) or C17 mimic the C_M – T responses in (A). Differences are noted at $T < T_M$ (local max/min vs plateau upon cooling below 44 °C), which are related to the effects of the lipid phase transition on alkane solvent solubility and organization in the bilayer. See Figures 1 and 2 for definitions of arrows and dashed boxes.

reduced solvent content in the bilayer,^{59,60} to better understand the role of the alkane solvent. Upon cooling these DIBs, C_M initially increased rapidly from 0.39 $\mu\text{F}/\text{cm}^2$ at 60 °C to 0.62 $\mu\text{F}/\text{cm}^2$ at 45 °C (Figure 4A), at which point the droplets became highly adhesive, an indication of high energy of adhesion (Figure S5). Below 45 °C, the bilayer area and capacitance were not easily altered by adjusting the position of the two droplets relative to each other, as could be done for the same bilayer at higher temperatures (or for fluid-phase DIBs, in general^{39,40}). The inability to mechanically induce changes in membrane capacitance or area at $T < 45$ °C suggests that C_M reached a stable maximum value of 0.615 $\mu\text{F}/\text{cm}^2$ and

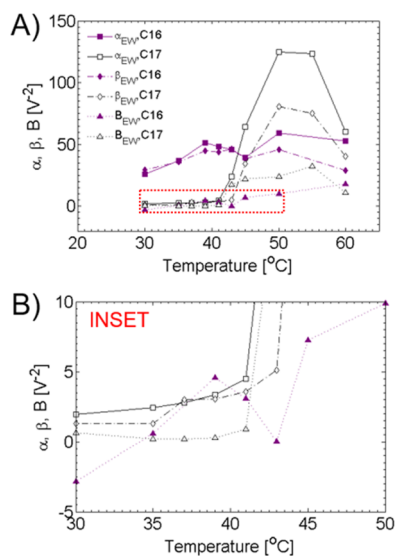


Figure 5. Electrowetting responses confirm the bTLE phase transition and alkane solvent effects. (A, B) constants (refer to text and equations) were measured at various temperatures while cooling bTLE DIBs in C16 or C17 alkane. The constants serve as an indicator of the sensitivity of the membrane to voltage-induced areal expansion (β_{EW}) and thinning (B_{EC}), both of which contribute to the total capacitive electrowetting response (α_{EW}). (B) shows the inset from (A) with scaled axes to allow the visualization of low-temperature behavior.

consequently a minimum d_{HC} value of 31.7 Å, consistent with the notion of nearly complete exclusion of the alkane solvent at lower temperatures.

Figure 4B shows nominal C – T curves for bTLE bilayers in C16 and C17 solvent. For both bilayers, cooling initially caused an increase in capacitance until the phase transition was reached, which we attribute to a decrease in solvent content. For bTLE/C16, the capacitance then decreased from a local maximum to a local minimum (also seen in C_M measurements shown in Figure 4A) as a result of an increase in the bilayer hydrophobic thickness. In contrast, bTLE/C17 bilayers showed a plateau in C – T and C_M – T curves below 44 $^{\circ}C$. Together, these results suggest that specific capacitance changes for bTLE/C16 are due to solvent reorganization (as opposed to a change in individual lipid area or length), whereas C_M values for bTLE/C17 DIBs indicate that the membrane contains less solvent below the transition. This interpretation is also consistent with DSC and density measurements that show only smooth, gradual changes in the ensemble-average lipid geometry (i.e., continuous excess specific heat that is directly proportional to the lipid volume, area, and length^{61,62}) in solvent-free bTLE vesicles.

The presence of excess oil in the membrane was further revealed by examining membrane responses to dc bias voltages. It has previously been shown that the application of an electric field can remove excess solvent from planar bilayers through electrostriction^{63,64} and enlarge the area of contact between adhesive droplets via electrowetting.⁴⁰ The presence of oil in the membrane hydrophobic core makes it more compressible⁶⁴ and, because of its higher resting tension, causes a greater electrowetting sensitivity.⁴⁰ Nominal capacitance follows a quadratic dependence on applied voltage, described by⁶⁴

$$C(V) = C_0(1 + \alpha_{EW}V^2) \quad (1)$$

where C_0 is the nominal capacitance with zero electric field and α_{EW} is a constant quantifying the sensitivity of capacitance to the applied voltage, V . The bilayer area and specific capacitance follow quadratic relationships similar to voltage,

$$A(V) = A_0(1 + \beta_{EW}V^2) \quad (2)$$

$$C_M(V) = C_{M,0}(1 + B_{EC}V^2) \quad (3)$$

where β_{EW} represents the strength of the electrowetting-induced area change, B_{EC} describes the strength of the electrocompression-induced changes in specific capacitance, and A_0 and $C_{M,0}$ are the zero-bias values.⁶⁴

Figure 5A,B shows the electrowetting and electrocompression constants (α_{EW} , β_{EW} , and B_{EC}) for bTLE DIBs formed in C16 and C17 solvent. While α_{EW} and β_{EW} are determined from measurements of C and A , B_{EC} is calculated simply as $B_{EC} = \alpha_{EW} - \beta_{EW}$ (eq 4).⁶⁴ Further details regarding the measurement of α_{EW} , β_{EW} , and B_{EC} are found in the Supporting Information. bTLE/C16 exhibits a local maximum and minimum in α_{EW} between 39 and 45 $^{\circ}C$, with nonzero B_{EC} implying the presence of compressible solvent-rich regions in the bilayer both above, within, and below the phase transition. In striking contrast, B_{EC} (and α_{EW} and β_{EW}) values reduced to nearly zero in bTLE/C17 DIBs cooled from 50 to 40 $^{\circ}C$, which is confirmation that solvent was completely excluded from the bilayer upon cooling through the phase transition. This finding is consistent with the observed high energy of adhesion between droplets (adhesion energy and contact angles correlate with solvent exclusion⁶⁰) and the observed plateau in C_M and nominal C for bTLE in C17 at $T < 45$ $^{\circ}C$ (Figure 4A,B).

DISCUSSION

Capacitance Measurements Detect Lipid Phase Transitions in DIBs. We have shown that saturated single-component and three-component DIBs exhibit nonlinear changes in capacitance (nominal C and specific C_M) at temperatures that correspond to known phase transitions. In these systems, abrupt changes are also observed in DSC, PPC, and densitometry measurements of solvent-free liposomes. Such changes are consistent with a first-order phase transition in which the lipid geometry (i.e., volume, area, and length) changes in a manner that is proportional to the transition enthalpy.^{61,62} By analogy to these well-studied systems, we propose that the capacitance changes observed in natural bTLE membranes near 40 $^{\circ}C$ (Figure 2A) mark the onset of a lipid miscibility transition. Remarkably, other techniques were unable to resolve this transition, which appears to be higher order given the continuity of order parameters (molar volume/density, enthalpy, and related lipid geometry) measured as a function of temperature. Such higher-order transitions are found near critical points, including those associated with critical opalescence in binary mixtures, where matter exists simultaneously in different states that are difficult to distinguish from one another (i.e., vapor \leftrightarrow liquid or $Lo \leftrightarrow Ld$ lipid), thus resulting in a single unique state for the entire phase.^{65,66}

Visual evidence of phase separation GUVs or planar bilayers composed of DPPC/DPhPC/Chol,^{31,48,49} combined with results from deuterium NMR³¹ and the new evidence presented herein of a capacitive transition in planar bilayers formed from the same lipid composition, collectively support the idea that a morphological transition takes place in DPPC/DPhPC/Chol membranes, despite a near-zero enthalpy change (tested herein

with a 20/50/30 mol % composition). In this regard, it is interesting to consider the possibility that other low-enthalpy transitions exist in biomembranes, previously unmeasured by calorimetric-, density-, or molar-volume-based measurements but that can now be investigated with capacitance measurements.

Mechanism of Phase-Transition-Induced Capacitance Changes in DIBs. The qualitatively different capacitance behavior in DIBs compared to liposomes can be understood by considering the contribution from alkane molecules and their thermodynamically governed solubility in the bilayer hydrophobic region.⁶⁷ It is well known that the formation of an adhesive lipid bilayer between lipid-coated droplets is entropically driven. The formation of adhesive bilayer interfaces is driven by the combined favorability of greater lipid–lipid interactions occurring in a solvent-depleted region and the reduced level of organization imposed on the solvent as it exits the bilayer region and joins the bulk solvent.⁶⁸ As a result, subtle changes in the amount or organization of solvent in the membrane can be of low-enthalpy origin and yet still measurable via capacitance. Moreover, the relative solubility of the solvent in the lipid acyl chains dictates how much solvent can remain in the membrane at a given temperature.

Heating-induced thickening of planar bilayers formed in the presence of bulk alkane stems from the enhanced solubility of the alkane in the membrane that causes more solvent to remain in the bilayer hydrophobic region. C_M data reported here and elsewhere^{18,57} show that the equilibrium partitioning of solvent between the bulk and the lipid acyl chains follows a monotonic relationship with respect to temperature, at least when the bilayer is in a liquid disordered state and the solvent is in a liquid state. Our measurements show a unique response in bTLE DIBs, which upon increasing the alkane length by one carbon from C16 to C17 displays behavior suggesting that the phase transition excludes all alkane solvent from the membrane. Our observations suggest that transition-induced reorganization of the solvent is a major factor governing the capacitive detection of low-enthalpy phase transitions.

Interestingly then, the ability to detect low-enthalpy phase transitions using capacitance measurements hinges on the fact that some amount of solvent is present in the hydrophobic core of the membrane such that it can rearrange in response to structural changes of the phospholipids at the transition. Indeed, prior studies with single-component membranes have shown that capacitive-transitions no longer occur if the solvent is completely excluded at a temperature well above the lipid phase transition.¹⁸ Although some solvent is helpful, it is known that an excess of residual solvent in the bilayer can significantly alter or fully abolish the thermotropic transitions of lipids.⁵⁹ The transition temperatures identified herein from DIB capacitance measurements agree closely with those obtained on solvent-free membranes.^{31,45} Thus, we conclude that DIBs formed in tetradecane (C14) or hexadecane (C16) contain residual solvent in an amount that enables capacitive detection without drastically altering the underlying lipid phase behavior.

Nature of Phase Domains in bTLE. The molecular-level picture of the phase transition and related lateral reorganization in bTLE membranes is currently incomplete, especially when compared to the well-studied and understood behavior of phase separating ternary lipid compositions. Fluorescence microscopy of DPPC/DPhPC/Chol GUVs³¹ and planar bilayers^{48,49} reveals clear lipid separation into distinct Ld and Lo domains at temperatures below T_{misc} . However, no clear signs of such

microscale phase separation are seen in bTLE GUVs at low temperature (25 °C, Figure 2B). FRET measurements can resolve the miscibility transition in ternary DSPC/POPC/Chol membranes that yield nanoscopic domains (Figure 2D), yet no clear miscibility transition is seen in FRET measurements of bTLE (Figure 2E). The lack of an identifiable miscibility transition via FRET in bTLE membranes suggests that either (a) bTLE lipids are uniformly mixed, (b) phase separation occurs but the fluorescent probes partition equally between the coexisting phases at all temperatures, or (c) phase separation occurs but the resulting domains are smaller than the spatial resolution of the FRET measurement (5–10 nm for the probe pairs used in other membranes²⁶). Domains that are not detectable by FRET must be very small, perhaps only a few nanometers in diameter. At the molecular level, “ultra-nanodomains”⁵⁵ of this size are likely transient clusters composed of fewer than 5–10 lipid and/or cholesterol molecules (1 lipid $\sim 70 \text{ \AA}^2$, radius 8–9 Å, diameter ~ 1.6 – 1.8 \AA). Such clusters would more accurately be described as nonideal mixing within a single fluid phase.^{28,69,70}

Biological Implications. A more complete understanding of higher-order, low-enthalpy phase transitions in membranes comprised of natural mixtures is likely necessary to fully understand the function of cellular membranes. There is increasing evidence that natural membranes utilize phase separation for sorting and signal transduction, to control cytoskeletal attachment, or to alter membrane fluidity and diffusion or mechanical properties.^{1–6} Synthetic multicomponent lipid mixtures are capable of producing such phase separation in model membranes, but many binary and ternary mixed membranes have measurable transition enthalpy and often display spontaneous lipid-ion channel formation, a phenomenon that is attributed to increased amplitudes of thermal area and compressibility fluctuations that are proportional to the system excess specific heat.^{61,71–73} Unwanted pore formation and defects would be expected to increase the permeability of the membrane to water, ions, and small molecules. A smooth or continuous low-enthalpy miscibility transition, on the other hand, could provide the ability to spatially regulate membrane structure and organization at the micro- or nanoscale, without the presence of high-amplitude thermal fluctuations and pore-formation-related defects that occur in simpler mixtures near their main transition temperatures.^{71–74} Additionally, the compositional complexity of natural membranes may confer the ability to present phase-separated regions at the subcellular level without spontaneous demixing into large macroscopic phases.

Additional studies are also needed to determine if the phase behavior detect in bTLE bilayer via capacitance measurements stems simply from the high degree of heterogeneity (tens to hundreds of lipid types) or a specific class or type of lipid in the mixture (i.e., charged lipids, sterols, sphingolipids, cerebrosides, etc.). Experiments on bilayers composed of lipid extracts from various tissues or organisms will likely provide more information on how specific cell types tune membrane composition and properties and processes associated with the low-enthalpy phase behavior. Thus, we are continuing to examine the interplay between DIB composition, temperature, phase, solvent solubility and content, and the surface or line tensions that arise in the membrane.

■ CONCLUSIONS

Our experiments using DIBs in alkanes confirm what others have shown before with single-component black lipid membranes: that it is possible to detect thermotropic melting and miscibility transitions using capacitance (these can also be detected using other methods). However, for the first time we find that capacitance measurements are also able to detect more subtle temperature-dependent rearrangements in membranes containing mixtures of synthetic or natural lipids that undergo transitions that remain hidden when observed using standard techniques. The capacitive transitions that occur in single-component saturated DIBs occur at the same temperature as for solvent-free vesicles examined with calorimetry or density measurements. Capacitance measurements with ternary lipid mixtures known to phase separate reveal C - T transitions in the same temperature range detected by fluorescence microscopy in GUVs. The difference between capacitance measurements and the other commonly used techniques is that higher-order phase transitions are easily detectable, as was demonstrated with membranes formed from bTLE, a natural eukaryotic mixture of membrane lipids. The sensitivity of capacitance measurements to low-enthalpy, higher-order phase transitions is a result of the inverse relationship between capacitance and hydrophobic thickness, whereby small changes in thickness can result in large changes in capacitance.

Although our measurements reveal that the presence of alkane solvent does not significantly alter the transition temperature, i.e., comparing DIBs to solvent-free vesicles, the oil does in fact play a role in conferring the ability to detect otherwise low-enthalpy phase transitions with capacitance. Oil exclusion from DIBs and droplet-based emulsions is an entropically driven process that also affects the membrane tension state and hydrophobic thickness. Both factors affect the resulting area and capacitance of the membrane. Thus, we are able to measure capacitance changes, even in the case of low-enthalpy thermotropic transformation of membrane structure, due to solvent redistribution in the bilayer hydrophobic region. In fact, our data suggest that the presence of solvent in the membrane may help to amplify these measured changes in capacitance caused by lipid transitions. These novel findings thus motivate our continued efforts to explore the link between capacitance-temperature hysteresis and the kinetics of alkane solvent uptake and exclusion. The responsiveness of oil distribution to phase transitions may also carry significant implications for natural membranes that are continuously remodeled to control the composition and distribution of hydrophobic and amphiphilic biomolecules such as neutral lipids and fatty acids (for example, with lipid droplets and the natural maintenance of membrane composition^{75,76}).

■ MATERIALS AND METHODS

Phospholipids were obtained in powder form from Avanti Polar Lipids (Alabaster, AL) and stored at -20 °C until further use: DPhPC (1,2-diphytanoyl-*sn*-glycero-3-phosphocholine), DMPC (1,2-dimyristoyl-*sn*-glycero-3-phosphocholine), DPPC (1,2-dipalmitoyl-*sn*-glycero-3-phosphocholine), DSPC (1,2-distearoyl-*sn*-glycero-3-phosphocholine), DOPC (1,2-dioleoyl-*sn*-glycero-3-phosphocholine), POPC (1-palmitoyl-2-oleoyl-*sn*-glycero-3-phosphocholine), bTLE (brain total lipid extract, porcine), and cholesterol (ovine wool, >98%). Cholesterol used in GUV experiments was obtained from Nu Chek Prep (Elysian, NY). The following fluorescent dyes were used: BoDIPY-PC (1,2-(4,4-difluoro-5,7-dimethyl-4-bora-3a,4a-diaza-*s*-indacene-3-pentanoyl)-1-hexadecanoyl-*sn*-glycero-3-phosphocholine) and C12:0 DiI (1,1'-didodecyl-3,3,3',3'-tetramethylindocarbocyanine perchlorate) were

purchased from Invitrogen (Carlsbad, CA), and naphtho[2,3-*a*]pyrene and DHE (ergosta-5,7,9(11),22-tetraen-3 β -ol) were purchased from Sigma-Aldrich (St. Louis, MO). Buffer reagents (MOPS, NaCl, NaOH), alkanes (hexadecane and heptadecane), and chloroform were also obtained from Sigma-Aldrich.

DSC and DIB Lipid Preparation. For DSC and DIB experiments, powdered lipid was hydrated with aqueous buffer (100 mM NaCl and 10 mM MOPS, pH 7.4⁴⁶) to achieve MLV suspensions with a concentration of 2 mg/mL. For lipids and lipid mixtures with transition temperatures above room temperature, the suspension was heated after the hydration of the lipid powder (single-component and bTLE) or film (multicomponent mixtures). MLV suspensions were then stored at 4 °C until use in DSC measurements or were repeatedly thawed and frozen (5 \times total between ambient and -20 °C) before LUV preparation. For all cases except bTLE, LUVs were formed by extruding a thawed MLV suspension through 100-nm-pore polycarbonate track-etched membranes (NanoSizer, T&T Scientific) using a hand-held miniextruder. Solutions were passed through the extruder a total of 11 times. bTLE LUVs were formed by brief sonication (FS20D, Fisher Scientific) above 45 °C or by extrusion after rapid solvent exchange. bTLE LUVs prepared via sonication and solvent exchange/extrusion yielded DIBs with similar C - T transition behavior.

DSC Measurements. DSC measurements were made using a NanoDSC calorimeter from TA Instruments. In each DSC run, the sample contained an MLV suspension and the reference contained DI water. The sample lipid concentration was 2 mg/mL. Before loading MLV samples or DI water references, solutions were placed under vacuum for 15 min with a stir bar rotating at 600 rpm to remove air bubbles. The volumes of the sample and reference cell were identical (0.5 mL each). A fixed pressure of 3 atm was used in DSC scans to further reduce bubble formation. The DSC scan protocol was as follows: cooling and equilibrating at 0 or 10 °C for 10 min and then three heating and cooling cycles to 70 °C and back. The first, second, and third cycles had progressively slower scan rates of 1, 0.25, and 0.1 °C/min, respectively. Temperature was held for a 10 min equilibration period at each temperature end point during heating and cooling cycles.

DIB Formation and Characterization. Temperature control for DIB formation and characterization was implemented as described previously⁴⁶ with a slight modification. An elastomeric PDMS (Dow Corning) substrate was used to form a reservoir for the alkane solvent used in DIB formation. The PDMS substrate was placed inside of an aluminum heating shell designed for use with the working distance of a 4X objective on an inverted Olympus IX-51 microscope. Unlike previous tests where the thermocouple was inserted into the PDMS near the bilayer, the thermocouple was placed directly in the oil reservoir in a position that did not interfere with droplet positioning.

To prepare a DIB, 300 nL aqueous droplets of lipid solution (2 mg/mL lipids) were first dispensed by pipet onto two agarose-coated ball-tipped electrodes. Electrodes consisted of 50 μ m silver wire that were held briefly over a flame to create a ball-shaped tip. The ball-tipped silver electrodes were submerged in bleach for an hour to obtain a silver/silver chloride coating. Immediately before DIB trials, clean Ag/AgCl-coated electrodes were dipped 10 times into 0.75% molten agarose (A9539) dissolved in buffer. The agarose-coated electrodes were then fixed in micromanipulators (Kite-L and Kite-R, World Precision Instruments) that were used to manipulate the electrodes and resulting droplet positions. Several minutes were allowed for monolayer formation after pipetting droplets onto the electrodes under oil, and the droplets were then brought into contact using the micromanipulators. With adequate monolayer assembly, DIB formation occurred spontaneously within seconds or minutes of droplet contact. With inadequate monolayer assembly, the two droplets coalesced into one large volume. Transmembrane current through DIBs was measured using an Axopatch 200B patch clamp amplifier and a Digidata 1440 data acquisition system (Molecular Devices). Details regarding the confirmation of bilayer formation and measurement of membrane capacitance, specific capacitance, and electro-

wetting constants are found in the [Supporting Information](#) and elsewhere.^{40,46}

Gas Chromatography/Mass Spectrometry (GC/MS). Phospholipids were converted to fatty acid methyl esters (FAMES) via acid-catalyzed methanolysis. Briefly, 5–10 μL of an aqueous vesicle suspension (containing 20–100 μg total lipid) was dispensed into a $13 \times 100 \text{ mm}^2$ screw top glass culture tube, followed by the addition of 1 mL of methanolic HCl (1 M) prepared with concentrated HCl and methanol.⁷⁷ The sample was vortex mixed, sealed under Ar, and incubated at 85 $^\circ\text{C}$ for 1 h. After cooling to ambient temperature, 1 mL H_2O was added and the sample was vortexed. FAMES were extracted with 1 mL hexane and vigorous vortex mixing, followed by low-speed centrifugation ($500 \times g$) for 10 min. Finally, 800 μL of the upper (hexane) phase was transferred to an autosampler vial and brought to 1 mL with hexane, for injection into the GC column.

GC/MS analysis was performed on an Agilent 7890A gas chromatograph (Santa Clara, CA) with a 5975C mass-sensitive detector operating in electron-impact mode. An HP-5MS capillary column ($30 \text{ m} \times 0.25 \text{ mm}$, $0.25 \mu\text{m}$ film thickness) was used with a helium carrier at 1 mL/min and an inlet temperature of 270 $^\circ\text{C}$. A 1 μL aliquot of FAME dissolved in hexane was injected in splitless mode using an Agilent 7693A automatic liquid sampler. After sample injection, the following column temperature program was initiated: 2 min at 60 $^\circ\text{C}$, 20 $^\circ\text{C}/\text{min}$ to 285 $^\circ\text{C}$ followed by 2 min at 285 $^\circ\text{C}$, and 20 $^\circ\text{C}/\text{min}$ to 325 $^\circ\text{C}$ followed by 7 min at 325 $^\circ\text{C}$, for a total run time of 24.25 min. Total ion chromatogram peaks were assigned and integrated using GC/MSD ChemStation Enhanced Data Analysis software (Agilent Technologies, Santa Clara, CA).

Fluorescence Microscopy of GUVs. GUVs were prepared using the electroformation method,⁷⁸ modified as follows. Lipid mixtures (300 nmoles total) were prepared in 200 μL of chloroform, deposited onto indium tin oxide (ITO)-coated glass slides (Delta Technologies, Loveland, CO) preheated to 50 $^\circ\text{C}$, and uniformly spread across one end of the slide. Residual chloroform was then removed by placing the slides under vacuum for 2 h. An electroformation chamber was formed by separating the two slides with an O-ring filled with 30 mM sucrose. The assembled chamber was stabilized in a custom -built aluminum block that was heated to 55 $^\circ\text{C}$ in a dry block heater. Lipid films were swelled for 1 h at 55 $^\circ\text{C}$ in a 10 Hz, 1 Vpp ac field using a Wavetek Meterman FG2C function generator (Meterman, Everett, WA) and then incubated at 55 $^\circ\text{C}$ for 2 h, followed by cooling to ambient temperature over 3 h. Samples were harvested into microcentrifuge tubes using large-orifice pipet tips and imaged using an Eclipse Ti wide-field microscope (Nikon Instruments, Melville, NY) equipped with a $60\times 1.2 \text{ NA}$ water immersion objective. Sample chambers for GUV observation consisted of a no. 1.5 coverslip and a microscope slide separated with a silicone spacer (Sigma-Aldrich) of 0.25 mm thickness.

FRET Spectroscopy Measurements. Mixtures of lipids in chloroform were prepared in glass culture tubes using a glass syringe and repeating dispenser (Hamilton USA, Reno, NV). Fluorescent probe/lipid molar ratios were 1:200 (DHE), 1:1500 (BoDIPY-PC), and 1:2000 (C12:0-DiI). Samples contained 500 nmoles of lipid that was transferred to 1.0 mL of H_2O via rapid solvent exchange (RSE)⁷⁹ to produce lipid vesicles of low average lamellarity. Samples were further diluted by a factor of 20 in the cuvette for FRET measurements. Fluorescence data were collected between 20 and 60 $^\circ\text{C}$ using a Fluorolog-3 spectrofluorometer (Horiba Scientific, Edison, NJ). Additional details of FRET data collection and analysis are described elsewhere.⁵⁴

■ ASSOCIATED CONTENT

📄 Supporting Information

The Supporting Information is available free of charge on the [ACS Publications website](#) at DOI: [10.1021/acs.langmuir.7b02022](https://doi.org/10.1021/acs.langmuir.7b02022).

PPC and density measurement methods and results, bTLE acyl chain composition via GC/MS, fluorescence

micrographs of GUVs, details for measurements and calculations of capacitance, electrowetting constants, and data showing high bTLE DIB adhesion at $T < T_M$ (PDF)

■ AUTHOR INFORMATION

Corresponding Authors

*E-mail: collierpc@ornl.gov.

*E-mail: ssarles@utk.edu.

ORCID

Graham J. Taylor: [0000-0001-8833-7705](https://orcid.org/0000-0001-8833-7705)

Author Contributions

The manuscript was written through contributions of all authors, and all authors contributed equally. All authors have given approval to the final version of the manuscript.

Notes

The authors declare the following competing financial interest(s): G. Taylor is employed by T&T Scientific Corporation, a company that manufactures liposome preparation equipment that was used in this work.

■ ACKNOWLEDGMENTS

This manuscript has been authored by UT-Battelle, LLC, under contract no. DE-AC0500OR22725 with the U.S. Department of Energy. The United States Government retains and the publisher, by accepting the article for publication, acknowledges that the United States Government retains a nonexclusive, paid-up, irrevocable, worldwide license to publish or reproduce the published form of this manuscript, or allow others to do so, for United States Government purposes. J.K. and F.A.H. acknowledge support from Laboratory Directed Research and Development Program award 6074 and from DOE scientific user facilities. G.J.T. and F.A.H. also acknowledge financial support from the Joint Institute for Biological Sciences. G.J.T. and S.A.S. acknowledge funding and support from the Air Force Office of Scientific Research Basic Research Initiative (grant number FA9550-12-1-0464). DIB measurements were made at the University of Tennessee, Knoxville (UTK). DSC, PPC, densitometry, and FRET experiments and GC/MS analyses were performed at Oak Ridge National Laboratory (ORNL). GUV preparation and confocal microscopy were performed at Cornell University and ORNL. ORNL is managed by UT-Battelle, LLC, under U.S. Department of Energy (DOE) contract no. DE-AC05-00OR22725.

■ REFERENCES

- (1) Elson, E. L.; Fried, E.; Dolbow, J. E.; Genin, G. M. Phase separation in biological membranes: integration of theory and experiment. *Annu. Rev. Biophys.* **2010**, *39*, 207–226.
- (2) Brown, D. A.; London, E. Functions of lipid rafts in biological membranes. *Annu. Rev. Cell Dev. Biol.* **1998**, *14* (1), 111–136.
- (3) Jacobson, K.; Mouritsen, O. G.; Anderson, R. G. W. Lipid rafts: at a crossroad between cell biology and physics. *Nat. Cell Biol.* **2007**, *9* (1), 7–14.
- (4) Simons, K.; Toomre, D. Lipid rafts and signal transduction. *Nat. Rev. Mol. Cell Biol.* **2000**, *1* (1), 31–39.
- (5) Nicolson, G. L. The Fluid—Mosaic Model of Membrane Structure: Still relevant to understanding the structure, function and dynamics of biological membranes after more than 40 years. *Biochim. Biophys. Acta, Biomembr.* **2014**, *1838* (6), 1451–1466.
- (6) Honigsmann, A.; Sadeghi, S.; Keller, J.; Hell, S. W.; Eggeling, C.; Vink, R. A lipid bound actin meshwork organizes liquid phase separation in model membranes. *eLife* **2014**, *3*, [10.7554/eLife.01671](https://doi.org/10.7554/eLife.01671)

- (7) Rilfors, L.; Lindblom, G.; Wieslander, Å.; Christiansson, A. Lipid Bilayer Stability in Biological Membranes. In *Membrane Fluidity*, Kates, M.; Manson, L. A., Eds.; Springer US: Boston, MA, 1984; pp 205–245.
- (8) Steim, J. M.; Tourtellotte, M. E.; Reinert, J. C.; McElhaney, R. N.; Rader, R. L. Calorimetric Evidence for the Liquid-Crystalline State of Lipids in a Biomembrane. *Proc. Natl. Acad. Sci. U. S. A.* **1969**, *63* (1), 104–109.
- (9) Morein, S.; Andersson, A.-S.; Rilfors, L.; Lindblom, G. Wild-type *Escherichia coli* cells regulate the membrane lipid composition in a window between gel and non-lamellar structures. *J. Biol. Chem.* **1996**, *271* (12), 6801–6809.
- (10) Engelman, D. M. X-ray diffraction studies of phase transitions in the membrane of *Mycoplasma laidlawii*. *J. Mol. Biol.* **1970**, *47* (1), 115–117.
- (11) Engelman, D. M. Lipid bilayer structure in the membrane of *Mycoplasma laidlawii*. *J. Mol. Biol.* **1971**, *58* (1), 153–165.
- (12) Melchior, D. L.; Morowitz, H. J.; Sturtevant, J. M.; Tsong, T. Y. Characterization of the plasma membrane of *Mycoplasma laidlawii*. VII. Phase transitions of membrane lipids. *Biochim. Biophys. Acta, Biomembr.* **1970**, *219* (1), 114–122.
- (13) de Kruyff, B.; Demel, R. A.; dan Deenen, L. L. M. The effect of cholesterol and epicholesterol incorporation on the permeability and on the phase transition of intact *Acholeplasma laidlawii* cell membranes and derived liposomes. *Biochim. Biophys. Acta, Biomembr.* **1972**, *255* (1), 331–347.
- (14) Verkleij, A. J.; Ververgaert, P. H. J.; Van Deenen, L. L. M.; Elbers, P. F. Phase transitions of phospholipid bilayers and membranes of *Acholeplasma laidlawii* B visualized by freeze fracturing electron microscopy. *Biochim. Biophys. Acta, Biomembr.* **1972**, *288* (2), 326–332.
- (15) Langner, M.; Komorowska, M.; Koter, M.; Gomukiewicz, J. Phase transitions in spherical bilayer membranes prepared of bulk erythrocyte membrane lipids. *Gen. Physiol. Biophys.* **1984**, *3*, 521–526.
- (16) Antonov, V.; Anosov, A.; Norik, V.; Korepanova, E.; Smirnova, E. Electrical capacitance of lipid bilayer membranes of hydrogenated egg lecithin at the temperature phase transition. *Eur. Biophys. J.* **2003**, *32* (1), 55–59.
- (17) Boheim, G.; Hanke, W.; Eibl, H. Lipid phase transition in planar bilayer membrane and its effect on carrier- and pore-mediated ion transport. *Proc. Natl. Acad. Sci. U. S. A.* **1980**, *77* (6), 3403–3407.
- (18) White, S. H. Phase transitions in planar bilayer membranes. *Biophys. J.* **1975**, *15*, 95–117.
- (19) Gliozzi, A.; Rolandi, R.; De Rosa, M.; Gambacorta, A. Monolayer black membranes from bipolar lipids of archaeobacteria and their temperature-induced structural changes. *J. Membr. Biol.* **1983**, *75* (1), 45–56.
- (20) Lee, D. E.; Lew, M. G.; Woodbury, D. J. Vesicle fusion to planar membranes is enhanced by cholesterol and low temperature. *Chem. Phys. Lipids* **2013**, *166*, 45–54.
- (21) Seeger, H. M.; Aldrovandi, L.; Alessandrini, A.; Facci, P. Changes in Single K⁺ Channel Behavior Induced by a Lipid Phase Transition. *Biophys. J.* **2010**, *99* (11), 3675–3683.
- (22) Naumowicz, M.; Figaszewski, Z. A. Impedance Analysis of Lipid Domains in Phosphatidylcholine Bilayer Membranes Containing Ergosterol. *Biophys. J.* **2005**, *89* (5), 3174–3182.
- (23) Naumowicz, M.; Figaszewski, Z. A. Impedance Analysis of Phosphatidylcholine/ α -Tocopherol System in Bilayer Lipid Membranes. *J. Membr. Biol.* **2005**, *205* (1), 29–36.
- (24) Naumowicz, M.; Petelska, A. D.; Figaszewski, Z. A. Impedance analysis of phosphatidylcholine–cholesterol system in bilayer lipid membranes. *Electrochim. Acta* **2005**, *50* (10), 2155–2161.
- (25) Naumowicz, M.; Petelska, A. D.; Figaszewski, Z. A. Impedance analysis of a phosphatidylcholine–phosphatidylethanolamine system in bilayer lipid membranes. *Electrochim. Acta* **2006**, *51* (24), 5024–5028.
- (26) Naumowicz, M.; Petelska, A. D.; Figaszewski, Z. A. Physicochemical analysis of phosphatidylcholine–ceramide system in bilayer lipid membranes. *Acta Biochim. Polonica* **2008**, *55*, 721–730.
- (27) Naumowicz, M.; Petelska, A. D.; Figaszewski, Z. A. Impedance Analysis of Complex Formation Equilibria in Phosphatidylcholine Bilayers Containing Decanoic Acid or Decylamine. *Cell Biochem. Biophys.* **2011**, *61* (1), 145–155.
- (28) Heberle, F. A.; Feigenson, G. W. Phase separation in lipid membranes. *Cold Spring Harbor Perspect. Biol.* **2011**, *3* (4), a004630.
- (29) Lewis, R.; Sykes, B. D.; McElhaney, R. N. Thermotropic phase behavior of model membranes composed of phosphatidylcholines containing cis-monounsaturated acyl chain homologues of oleic acid: differential scanning calorimetric and ³¹P NMR spectroscopic studies. *Biochemistry* **1988**, *27* (3), 880–887.
- (30) Veatch, S. L.; Soubias, O.; Keller, S. L.; Gawrisch, K. Critical fluctuations in domain-forming lipid mixtures. *Proc. Natl. Acad. Sci. U. S. A.* **2007**, *104* (45), 17650–17655.
- (31) Veatch, S. L.; Gawrisch, K.; Keller, S. L. Closed-Loop Miscibility Gap and Quantitative Tie-Lines in Ternary Membranes Containing Diphytanoyl PC. *Biophys. J.* **2006**, *90* (12), 4428–4436.
- (32) Nickels, J. D.; Chatterjee, S.; Stanley, C. B.; Qian, S.; Cheng, X.; Myles, D. A. A.; Standaert, R. F.; Elkins, J. G.; Katsaras, J. The in vivo structure of biological membranes and evidence for lipid domains. *PLoS Biol.* **2017**, *15* (5), e2002214.
- (33) Wu, H.-L.; Tong, Y.; Peng, Q.; Li, N.; Ye, S. Phase transition behaviors of the supported DPPC bilayer investigated by sum frequency generation (SFG) vibrational spectroscopy and atomic force microscopy (AFM). *Phys. Chem. Chem. Phys.* **2016**, *18* (3), 1411–1421.
- (34) Scomparin, C.; Lecuyer, S.; Ferreira, M.; Charitat, T.; Tinland, B. Diffusion in supported lipid bilayers: Influence of substrate and preparation technique on the internal dynamics. *Eur. Phys. J. E: Soft Matter Biol. Phys.* **2009**, *28* (2), 211–220.
- (35) Sterling, S. M.; Dawes, R.; Allgeyer, E. S.; Ashworth, S. L.; Neivandt, D. J. Comparison of Actin- and Glass-Supported Phospholipid Bilayer Diffusion Coefficients. *Biophys. J.* **2015**, *108* (8), 1946–1953.10.1016/j.bpj.2015.02.033
- (36) Goksu, E. I.; Longo, M. L. Ternary Lipid Bilayers Containing Cholesterol in a High Curvature Silica Xerogel Environment. *Langmuir* **2010**, *26* (11), 8614–8624.
- (37) Seeger, H. M.; Cerbo, A. D.; Alessandrini, A.; Facci, P. Supported Lipid Bilayers on Mica and Silicon Oxide: Comparison of the Main Phase Transition Behavior. *J. Phys. Chem. B* **2010**, *114* (27), 8926–8933.
- (38) Bayley, H.; Cronin, B.; Heron, A.; Holden, M. A.; Hwang, W. L.; Syeda, R.; Thompson, J.; Wallace, M. Droplet interface bilayers. *Mol. Biosyst.* **2008**, *4* (12), 1191–1208.
- (39) Gross, L. C. M.; Heron, A. J.; Baca, S. C.; Wallace, M. I. Determining Membrane Capacitance by Dynamic Control of Droplet Interface Bilayer Area. *Langmuir* **2011**, *27* (23), 14335–14342.
- (40) Taylor, G. J.; Venkatesan, G. A.; Collier, C. P.; Sarles, S. A. Direct in situ measurement of specific capacitance, monolayer tension, and bilayer tension in a droplet interface bilayer. *Soft Matter* **2015**, *11* (38), 7592–7605.
- (41) Lewis, R. N. A. H.; Mak, N.; McElhaney, R. N. A differential scanning calorimetric study of the thermotropic phase behavior of model membranes composed of phosphatidylcholines containing linear saturated fatty acyl chains. *Biochemistry* **1987**, *26* (19), 6118–6126.
- (42) Lindsey, H.; Petersen, N. O.; Chan, S. I. Physicochemical characterization of 1,2-diphytanoyl-sn-glycero-3-phosphocholine in model membrane systems. *Biochim. Biophys. Acta, Biomembr.* **1979**, *555* (1), 147–167.
- (43) Konyakhina, T. M.; Wu, J.; Mastroianni, J. D.; Heberle, F. A.; Feigenson, G. W. Phase diagram of a 4-component lipid mixture: DSPC/DOPC/POPC/chol. *Biochim. Biophys. Acta, Biomembr.* **2013**, *1828* (9), 2204–2214.
- (44) Konyakhina, T. M.; Goh, S. L.; Amazon, J.; Heberle, F. A.; Wu, J.; Feigenson, G. W. Control of a Nanoscopic-to-Macroscopic Transition: Modulated Phases in Four-Component DSPC/DOPC/POPC/Chol Giant Unilamellar Vesicles. *Biophys. J.* **2011**, *101* (2), L8–L10.

- (45) Heberle, F. A.; Petruzielo, R. S.; Pan, J.; Drazba, P.; Kučerka, N.; Standaert, R. F.; Feigenson, G. W.; Katsaras, J. Bilayer Thickness Mismatch Controls Domain Size in Model Membranes. *J. Am. Chem. Soc.* **2013**, *135* (18), 6853–6859.
- (46) Taylor, G. J.; Sarles, S. A. Heating-Enabled Formation of Droplet Interface Bilayers Using *Escherichia coli* Total Lipid Extract. *Langmuir* **2015**, *31* (1), 325–337.
- (47) Yanagisawa, M.; Yoshida, T.-a.; Furuta, M.; Nakata, S.; Tokita, M. Adhesive force between paired microdroplets coated with lipid monolayers. *Soft Matter* **2013**, *9*, 5891–5897.
- (48) Collins, M. D.; Keller, S. L. Tuning lipid mixtures to induce or suppress domain formation across leaflets of unsupported asymmetric bilayers. *Proc. Natl. Acad. Sci. U. S. A.* **2008**, *105* (1), 124–128.
- (49) Danial, J. S. H.; Cronin, B.; Mallick, C.; Wallace, M. I. On demand modulation of lipid composition in an individual bilayer. *Soft Matter* **2017**, *13* (9), 1788–1793.
- (50) Needham, D.; Evans, E. Structure and mechanical properties of giant lipid (DMPC) vesicle bilayers from 20.degree.C below to 10.degree.C above the liquid crystal-crystalline phase transition at 24.degree.C. *Biochemistry* **1988**, *27* (21), 8261–8269.
- (51) Radhakrishnan, A. Phase Separations in Binary and Ternary Cholesterol-Phospholipid Mixtures. *Biophys. J.* **2010**, *98* (9), L41–L43.
- (52) Baumgart, T.; Hunt, G.; Farkas, E. R.; Webb, W. W.; Feigenson, G. W. Fluorescence probe partitioning between Lo/Ld phases in lipid membranes. *Biochim. Biophys. Acta, Biomembr.* **2007**, *1768* (9), 2182–2194.
- (53) Petruzielo, R. S.; Heberle, F. A.; Drazba, P.; Katsaras, J.; Feigenson, G. W. Phase behavior and domain size in sphingomyelin-containing lipid bilayers. *Biochim. Biophys. Acta, Biomembr.* **2013**, *1828* (4), 1302–1313.
- (54) Heberle, F. A.; Wu, J.; Goh, S. L.; Petruzielo, R. S.; Feigenson, G. W. Comparison of Three Ternary Lipid Bilayer Mixtures: FRET and ESR Reveal Nanodomains. *Biophys. J.* **2010**, *99* (10), 3309–3318.
- (55) Pathak, P.; London, E. The Effect of Membrane Lipid Composition on the Formation of Lipid Ultrananodomains. *Biophys. J.* **2015**, *109* (8), 1630–1638.
- (56) Buboltz, J. T. Steady-state probe-partitioning fluorescence resonance energy transfer: a simple and robust tool for the study of membrane phase behavior. *Phys. Rev. E* **2007**, *76* (2), 021903.
- (57) White, S. H. Temperature-dependent structural changes in planar bilayer membranes: Solvent “freeze-out”. *Biochim. Biophys. Acta, Biomembr.* **1974**, *356* (1), 8–16.
- (58) Kučerka, N.; Nieh, M.-P.; Katsaras, J. Fluid phase lipid areas and bilayer thicknesses of commonly used phosphatidylcholines as a function of temperature. *Biochim. Biophys. Acta, Biomembr.* **2011**, *1808* (11), 2761–2771.
- (59) McIntosh, T. J.; Simon, S. A.; MacDonald, R. C. The organization of n-alkanes in lipid bilayers. *Biochim. Biophys. Acta, Biomembr.* **1980**, *597* (3), 445–463.
- (60) Needham, D.; Haydon, D. A. Tensions and free energies of formation of “solventless” lipid bilayers. Measurement of high contact angles. *Biophys. J.* **1983**, *41* (3), 251–257.
- (61) Heimburg, T. Mechanical aspects of membrane thermodynamics. Estimation of the mechanical properties of lipid membranes close to the chain melting transition from calorimetry. *Biochim. Biophys. Acta, Biomembr.* **1998**, *1415* (1), 147–162.
- (62) Heimburg, T. The capacitance and electromechanical coupling of lipid membranes close to transitions: the effect of electrostriction. *Biophys. J.* **2012**, *103* (5), 918–929.
- (63) White, S. Formation of “solvent-free” black lipid bilayer membranes from glyceryl monooleate dispersed in squalene. *Biophys. J.* **1978**, *23* (3), 337–347.
- (64) White, S.; Chang, W. Voltage dependence of the capacitance and area of black lipid membranes. *Biophys. J.* **1981**, *36* (2), 449.
- (65) Kunieda, H.; Frigeri, S. E. Critical Phenomena in a Surfactant/Water/Oil System. Basic Study on the Correlation between Solubilization, Microemulsion, and Ultralow Interfacial Tensions. *Bull. Chem. Soc. Jpn.* **1981**, *54* (4), 1010–1014.
- (66) Cheung, A. Phase transitions and collective phenomena. *Lecture Notes* **2011**, 5–9.
- (67) White, S. H. The lipid bilayer as a ‘solvent’ for small hydrophobic molecules. *Nature* **1976**, *262* (5567), 421–422.
- (68) Poulin, P.; Bibette, J. Adhesion of water droplets in organic solvent. *Langmuir* **1998**, *14* (22), 6341–6343.
- (69) Ackerman, D. G.; Feigenson, G. W. Lipid bilayers: clusters, domains and phases. *Essays Biochem.* **2015**, *57*, 33–42.
- (70) London, E. How principles of domain formation in model membranes may explain ambiguities concerning lipid raft formation in cells. *Biochim. Biophys. Acta, Mol. Cell Res.* **2005**, *1746* (3), 203–220.
- (71) Heimburg, T. Lipid ion channels. *Biophys. Chem.* **2010**, *150* (1–3), 2–22.
- (72) Blicher, A.; Wodzinska, K.; Fidorra, M.; Winterhalter, M.; Heimburg, T. The temperature dependence of lipid membrane permeability, its quantized nature, and the influence of anesthetics. *Biophys. J.* **2009**, *96* (11), 4581–4591.
- (73) Antonov, V. F.; Petrov, V. V.; Molnar, A. A.; Predvoditelev, D. A.; Ivanov, A. S. The appearance of single-ion channels in unmodified lipid bilayer membranes at the phase transition temperature. *Nature* **1980**, *283* (5747), 585–586.
- (74) Marquardt, D.; Heberle, F. A.; Miti, T.; Eicher, B.; London, E.; Katsaras, J.; Pabst, G. 1H NMR Shows Slow Phospholipid Flip-Flop in Gel and Fluid Bilayers. *Langmuir* **2017**.33373110.1021/acs.langmuir.6b04485
- (75) Wang, C.-W. Lipid droplets, lipophagy, and beyond. *Biochim. Biophys. Acta, Mol. Cell Biol. Lipids* **2016**, *1861*, 793–805.
- (76) Pol, A.; Gross, S. P.; Parton, R. G. Biogenesis of the multifunctional lipid droplet: Lipids, proteins, and sites. *J. Cell Biol.* **2014**, *204* (5), 635–646.
- (77) Ichihara, K. i.; Fukubayashi, Y. Preparation of fatty acid methyl esters for gas-liquid chromatography. *J. Lipid Res.* **2010**, *51* (3), 635–640.
- (78) Angelova, M.; Soleau, S.; Méléard, P.; Faucon, F.; Bothorel, P. Preparation of giant vesicles by external AC electric fields. Kinetics and applications. In *Trends in Colloid and Interface Science VI*; Springer, 1992; pp 127–131.
- (79) Buboltz, J. T.; Feigenson, G. W. A novel strategy for the preparation of liposomes: rapid solvent exchange. *Biochim. Biophys. Acta, Biomembr.* **1999**, *1417* (2), 232–245.